This document is the unedited Author's version of a Submitted Work that was subsequently accepted for publication in ACS Applied Energy Materials, copyright © American Chemical Society after peer review. To access the final edited and published work see DOI: 10.1021/acsaem.9b01887

Accelerated Screening of High Energy Li-Ion

Battery Cathodes

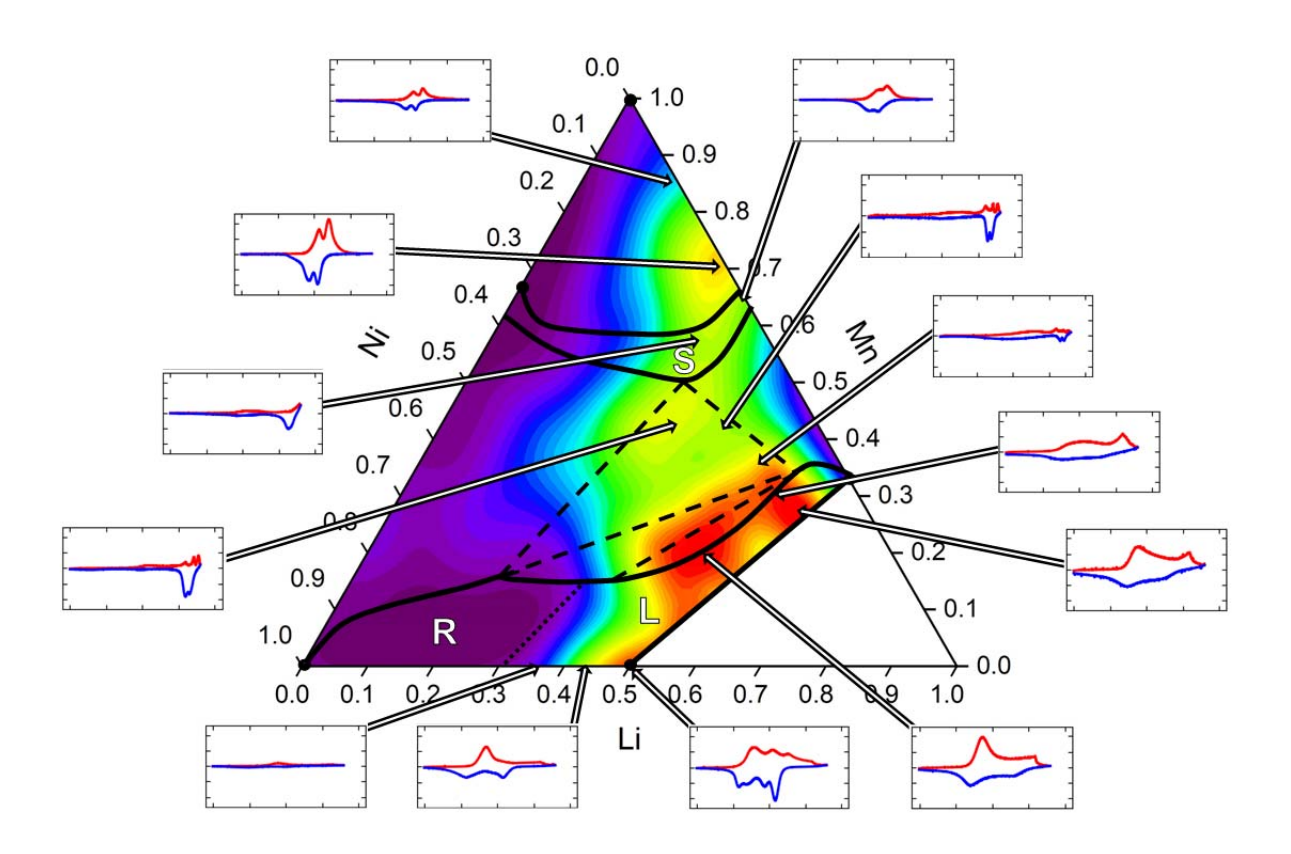
Karlie P. Potts, Eloi Grignon, and Eric McCalla*

Department of Chemistry, McGill University, Montreal, Canada

ABSTRACT

The need for better battery materials has driven research into under-explored complex phase spaces. Herein, we perform the first high-throughput electrochemical study of the entire Li-Ni-Mn-O system of interest for next-generation high-energy cathodes. We first adapt a high-throughput electrochemical system to cycle 64 mg-scale cathodes simultaneously and demonstrate its effectiveness with 2 test materials: LiCoO₂ and Li[Ni_{1/3}Mn_{1/3}Co_{1/3}]O₂. The average values for the electrochemical properties obtained for the combinatorial samples show excellent agreement with literature and cell-to-cell reproducibility is about 7%. The results for the Li-Ni-Mn-O system deepens our understanding dramatically and will guide the rational design of high-energy cathodes.

TOC GRAPHIC



KEYWORDS

Combinatorial synthesis, Li-ion cathode, electrochemical characterization, Li-Mn-Ni-O pseudoternary system,

Introduction

In the on-going search for higher energy cathode materials, the compositional complexity has increased dramatically. Whereas the first commercialized Li-ion batteries used LiCoO₂ (LCO) as the cathode material, cathodes produced today for applications such as electric vehicles (EVs) are typically pseudo-quaternary oxides, in which some of the Co atoms are replaced to yield Li[Ni,Mn,Co]O₂ (NMC) or Li[Ni,Al,Co]O₂ (NCA). Over the past 30 years, these advances have contributed to a dramatic increase in safety, energy density, and lifetime of the battery all the while decreasing the cost. However, such complex quaternary systems remain primarily unexplored with only select compositions having been investigated electrochemically.^{2,3} Therefore, there remains a strong need for higher throughput in the electrochemical studies of Liion cathodes.

There have been considerable efforts to use high-throughput computation to identify candidates for promising battery materials (cathodes, anodes, and solid electrolytes). Hollie these methods have proved very powerful, there are limitations to their predictions. Present computational methods struggle to account for solid-solutions, as the size of the supercell would become unmanageable in cases where small variations in stoichiometry impact performance. It also continues to be challenging to predict which metastable phases are stabilized at high temperatures, which is critical in battery materials where many commercially relevant syntheses occur at high temperatures. These limitations of high-throughput computation are well illustrated by recent combinatorial experimental work of the Dahn group. Through a combination of high-throughput synthesis and X-ray diffraction (XRD), the complete structural phase diagrams for the Li-Ni-Mn-Co-O pseudo-quaternary system were mapped out under various synthetic conditions. Results from these studies demonstrated that: (i) the phase diagrams are

extremely complex and exhibit large single phase regions, (ii) the electrochemistry, though only studied on select compositions, varies dramatically within the single phase regions, and (iii) structural changes occurring during slow cooling also impact the electrochemistry. 10,11 At the current time, these key observations would have been very difficult to predict using only a computational approach. While this work demonstrated the significant potential of combinatorial work on cathode materials, it was limited by the lack of high-throughput electrochemistry,³ and this is also the case for more recent work performed at Argonne National Laboratories. 12 As such, the electrochemical consequences of the structural phase diagrams have not been elucidated and no comprehensive structure-property relation exists for these critical materials. In fact, to date, high-throughput electrochemistry of battery materials has been limited to thin films¹³⁻¹⁸ and to the optimization of electrode formulation¹⁹⁻²¹ rather than the characterization of vast active material compositions. While the screening of thin film layered oxides (including the materials studied herein) is important, it solely serves to develop thin film batteries, as results do not match up well to that seen in bulk powders as used commercially in high-energy applications such as EVs.²² This is mainly due to: (i) the surface area/volume ratio being vastly different resulting in dramatically altered long-term cycling, and (ii) the control of oxygen content is very challenging such that preparing a sample array of thin films that shows the same structures as those obtained in bulk powders has, to date, proven impossible. ^{22,23}

The current study therefore aims to adapt a combinatorial system that works well for thin film anodes in such a way to investigate 64 powder cathode materials simultaneously. The system that was adapted was designed by the Dahn group, wherein thin film alloys were tested as anodes. ^{13,14,24} The measurements used a 64-sample combinatorial cell in which the samples were sputtered onto a printed circuit board (PCB) containing 64 nickel pads. The cell was then

assembled with a thin electrolyte-soaked separator and a single piece of lithium that would serve as a counter and reference electrode. This resulted in 64 cells connected in parallel, such that cyclic voltammetry could be performed on all samples at the same time, enabling the simultaneous monitoring of capacity, average voltage, irreversible capacity and capacity fade across entire ternary systems. ^{13,16,17}

The first objective of the current study is therefore to adapt this cell designed for thin films operating near 0-1 V vs. Li for use on 2 mg powders operating as high as 5 V. Figure 1A shows the adapted electrochemical cell wherein changes were made to each of the current collectors, the separator material and the manner in which the cell was sealed. The details of this development are described in detail in the S.I. section S2. The final design involves adhering aluminum foil to the printed circuit board using electrochemically stable materials, using two thick separators in order to apply stack pressure to all 64 cells at once, and to use a thick polymeric sealing membrane to make the seal. Figure S2B shows that this cell is stable to 5.0 V (no more than 10 µA of background current) such that screening of active materials in the range 3.0 V - 5.0 V can be readily done with this cell design. The final challenge in performing the high-throughput electrochemistry relates to preparing 64 electrodes efficiently while avoiding contamination between neighboring cells and accurately measuring the masses of all 64 active materials. The procedure, detailed in the S.I., involved first weighing each active material, mixing them with carbon black on the printed circuit board and then drop casting NMP with PVDF dissolved in it onto the powders. The result, after approximately 2 h of work, are 64 electrodes containing approximately 70% active materials as well as both conductive carbon black and PVDF binder. This electrode formulation is similar to that used commercially, though we increase significantly the amount of conductive additive due to the limited amount of mixing

that can be done with the small combinatorial samples. The validation of this electrode formulation was performed by making cells with two test materials (LCO and NMC) arranged in checkerboard fashion. Given that the two materials demonstrate starkly different electrochemical profiles it is easy to identify any contamination between neighboring cells as illustrated in Fig. S4. Figure 2 clearly shows no such contamination occurs. Furthermore, Figure 1B shows that the CVs obtained here are in good agreement with data obtained from bulk samples using coin cells in the literature. 25,26 The slight hysteresis and peak broadening present in the combinatorial data compared to the literature is attributed to reduced conductivity in the electrodes given the limited mixing with carbon black that our procedure allows.²⁷ Despite this, the deviation in peak positions is typically limited to 20 mV compared to literature on charge and less than 5 mV on discharge. Table 1 shows battery properties extracted for each of the test materials in a single combinatorial cell (32 samples of each) along with those obtained from literature under similar cycling conditions. ^{28–31} The average specific capacities were within 2.6% of that obtained for bulk samples, while the average voltages were within 1.5%. This demonstrates a high level of precision in the combinatorial measurements. Furthermore, the standard deviations for average voltage are negligible, while those for specific capacities are both near 7.5% showing good reproducibility amongst the 2 mg samples. Given that the uncertainty on the weighing of such small samples is approximately 5%, these low standard deviations are commendable, and we consider these to be optimal. Such low standard deviations and overall agreement with bulk methods allows us to now confidently use this system to screen systematically across compositions. This demonstrated quantitative agreement between the electrochemistry of LCO and NMC in our mg-scale combinatorial cell and traditional cells made

with bulk materials also confirms that our findings in the combinatorial studies will scale-up well.

The first combinatorial electrochemical results for the entire Li-Mn-Ni-O ternary system are therefore presented here. As detailed in the S.I. section S3, three plates of 64 samples were synthesized and cycled in the range 3.0 - 4.4 V for the first cycle with further cycling in the range 3.0 – 4.8 V. The first cycle serves to screen traditional layered oxides (LiMO₂) which show activity below 4.4 V, while the subsequent cycles screen for Li-rich layered materials $(Li_{1+x}M_{1-x}O_2)$ which show significant activation above 4.5 V. The synthesis and cycling of the 192 samples all took place in a 1-week period performed by a single researcher and the raw data is all included in the supplemental information. It is of note that the cooling method selected for the samples was slow cooling (quenching dramatically changes the phase diagram, but this method is not typically used commercially). Figure 3 shows both the energy density during discharge from 4.8 to 3.0 V and the structural phase diagram reported for the same synthesis conditions.9 Figure S6B highlights specific compositions to help situate the reader to this particular ternary diagram. Key electrochemical curves (both the cyclic voltammograms and the corresponding voltage vs. capacity plots) are also shown in Fig. 3 to visually demonstrate the progression of the battery performance as compositions vary. Figure 4 shows the progression of other important electrochemical properties in the system. Several structure-property trends between electrode composition and electrochemical performance now become evident. S.I. section S4 discusses such trends in the spinel region, while here we focus on the layered materials that are of highest interest for next-generation batteries. Regarding the layered materials, Fig. 3E-G shows the rapid increase in observed electrochemical activity as compositions move into the layered region. While this is understood in the literature, what is not

so thoroughly understood is the progression of properties within the layered region (this is a 2D region in the phase diagram, studies have typically emphasized a single line between Li₂MnO₃ and LiNi_{1/2}Mn_{1/2}O₂).³² The key trends visible in Figs. 3 and 4 include: (i) higher Ni content in the layered structures leads to higher capacities up to 4.4 V but after activation of the Li-rich regions both Ni-rich (Fig. 3H) and Mn-rich (Fig. 3I-J) compositions show high discharge capacities nearing 200 mAh/g, (ii) the average voltage shows only small variations with composition in the layered region, (iii) voltage fade (drop in average voltage between subsequent cycles) is more significant in the region with more Mn, and (iv) irreversible capacity (difference between first charge and first discharge capacity) seen in Li-rich oxides varies dramatically with composition (Figs. 3I,J,H). Thus, in terms of screening for the best cathodes, Fig. 3 shows that I, J, and H all show high energy densities of about 700 mWh/g, however H shows the lowest irreversible capacities. These results clearly suggest that further exploration of the region around sample H is warranted. Overall, the data here clearly shows that we now have the capability to track the properties required to discover optimal cathodes, including irreversible capacity, which relates to the amount of irreversible oxygen gas produced during activation of the Li-rich oxide. Furthermore, the value of 5 mV/cycle found here for the voltage fade of composition I (Fig. 4D) is comparable to that of 2.1 ± 1.7 mV/cycle reported in literature for a similar composition³³. Voltage fade and high irreversible capacities are the two key properties currently limiting the commercialization of Li-rich oxides,³⁴ implying that the methodology used here can now be used to optimize these important properties. It should be noted that under galvanostatic conditions the high voltage plateau requires as much as 50 h to fully activate, 32 it is therefore expected that a thorough study of this region under various cycling conditions (here the cells spent 10 h on this plateau only) will be essential to find the optimum Li-rich oxide. An important on-going aspect of this research is therefore to expand the search to the entire pseudo-quaternary Li-Ni-Mn-Co-O and Li-Ni-Co-Al-O systems of highest immediate interest with a particular focus on Li-rich compositions to be studied under various cycling conditions guided by the current results.

Furthermore, composite layered-spinel cathodes have been proposed as potential next-generation cathodes, ^{35,36} though there remains no clear understanding of how the battery properties of the composites compare to the weighted average of the two component phases. More specifically, for a composite to outperform both end-member materials there must be a synergistic effect resulting in a property not simply being a linear combination of the two end-members' properties. This can now be readily evaluated in Figs. 3-4 for some key metrics. As seen in Fig. 4A-C, both capacity and average voltage do progress monotonically along tie-lines implying no synergistic effect is present. These trends also apply to materials in the 3-phase regions (Figs. 3D,L, and K all lie in a 3-phase region), though one must recognize that under the synthesis conditions used much of the 3-phase regions in fact contain 4-phases because equilibrium states are not reached at moderate cooling rates. ⁹ Although composites do not seem to have benefits with regards to energy density, it remains to be seen whether there could be some benefit to long term cycling and further study is required in this regards.

In this work, we demonstrate a high-throughput electrochemical testing system adapted for the investigation of high-energy cathode materials. The level of precision and accuracy achieved by the system provides the capability to study important electrochemical parameters including capacity, average working voltage, energy, and voltage fade between cycles. These performance metrics were examined across the entire Li-Mn-Ni-O pseudo-ternary system in a single week's time and represents the first high-throughput screening of powder cathode materials. Key properties for next-generation cathodes, including energy density, irreversible capacity, capacity,

and voltage fade (over approximately 10 cycles), can now all be efficiently monitored in ternary

and quaternary composition spaces such as the entire NMC and NCA systems. This research

now opens up numerous avenues to not only rapidly screen potential battery materials but to

develop meaningful structure-property relations that are badly needed for the rational design of

advanced battery materials.

ASSOCIATED CONTENT

*Corresponding author: eric.mccalla@mcgill.ca

Supporting Information.

Supplemental text (S1 Experimental Methods, S2 Further details regarding adaptations and

validation of the combinatorial cell, S3. Data treatment for the Li-Mn-Ni-O pseudo-ternary

system, and S4. Discussion regarding the electrochemistry in the spinel region), Figures S1-S13.

Notes

The authors declare no competing financial interest.

ACKNOWLEDGMENT

This work was funded by the Natural Sciences and Engineering Research Council of Canada

under the auspices of a Discovery grant as well as an FRQNT new researcher grant. EG also

received funding from an NSERC USRA scholarship. The authors gratefully acknowledge Jeff

Dahn for supplying the combinatorial electrochemical system used in refs. 13,14,24

REFERENCES

Xiao, J.; Chernova, N. A.; Whittingham, M. S. Layered Mixed Transition Metal Oxide (1) Cathodes with Reduced Cobalt Content for Lithium Ion Batteries. Chem. Mater. 2008, 20

(24), 7454–7464. https://doi.org/10.1021/cm802316d.

10

- (2) Brown, C. R.; McCalla, E.; Watson, C.; Dahn, J. R. Combinatorial Study of the Li–Ni–Mn–Co Oxide Pseudoquaternary System for Use in Li–Ion Battery Materials Research. *ACS Comb. Sci.* **2015**, *17* (6), 381–391.
- (3) McCalla, E. Consequences of Combinatorial Studies of Positive Electrodes for Li-Ion Batteries; Springer Science & Business Media, 2014.
- (4) Jain, A.; Ong, S. P.; Hautier, G.; Chen, W.; Richards, W. D.; Dacek, S.; Cholia, S.; Gunter, D.; Skinner, D.; Ceder, G. Commentary: The Materials Project: A Materials Genome Approach to Accelerating Materials Innovation. *Apl Mater.* **2013**, *1* (1), 11002.
- (5) Jain, A.; Persson, K. A.; Ceder, G. Research Update: The Materials Genome Initiative: Data Sharing and the Impact of Collaborative Ab Initio Databases. *APL Mater.* **2016**, *4* (5), 53102.
- (6) Urban, A.; Seo, D.-H.; Ceder, G. Computational Understanding of Li-Ion Batteries. *npj Comput. Mater.* **2016**, *2*, 16002.
- (7) Hautier, G.; Fischer, C. C.; Jain, A.; Mueller, T.; Ceder, G. Finding Nature's Missing Ternary Oxide Compounds Using Machine Learning and Density Functional Theory. *Chem. Mater.* **2010**, 22 (12), 3762–3767.
- (8) Sun, W.; Dacek, S. T.; Ong, S. P.; Hautier, G.; Jain, A.; Richards, W. D.; Gamst, A. C.; Persson, K. A.; Ceder, G. The Thermodynamic Scale of Inorganic Crystalline Metastability. *Sci. Adv.* **2016**, *2* (11), e1600225.
- (9) McCalla, E.; Rowe, A. W.; Shunmugasundaram, R.; Dahn, J. R. Structural Study of the Li-Mn-Ni Oxide Pseudoternary System of Interest for Positive Electrodes of Li-Ion Batteries. *Chem. Mater.* **2013**, *25* (6), 989–999.
- (10) McCalla, E.; Rowe, A. W.; Brown, C. R.; Hacquebard, L. R. P.; Dahn, J. R. How Phase Transformations during Cooling Affect Li-Mn-Ni-O Positive Electrodes in Lithium Ion Batteries. *J. Electrochem. Soc.* **2013**, *160* (8), A1134–A1138.
- (11) McCalla, E.; Li, J.; Rowe, A. W.; Dahn, J. R. The Negative Impact of Layered-Layered Composites on the Electrochemistry of Li-Mn-Ni-O Positive Electrodes for Lithium-Ion Batteries. *J. Electrochem. Soc.* **2014**, *161* (4), A606–A613.
- (12) Vu, A.; Qin, Y.; Lin, C.-K.; Abouimrane, A.; Burrell, A. K.; Bloom, S.; Bass, D.; Bareño, J.; Bloom, I. Effect of Composition on the Voltage Fade Phenomenon in Lithium-, Manganese-Rich XLiMnO3·(1- x) LiNiaMnbCocO2: A Combinatorial Synthesis Approach. *J. Power Sources* **2015**, 294, 711–718.
- (13) Fleischauer, M. D.; Dahn, J. R. Combinatorial Investigations of the Si-Al-Mn System for Li-Ion Battery Applications. *J. Electrochem. Soc.* **2004**, *151* (8), A1216–A1221.
- (14) Fleischauer, M. D.; Topple, J. M.; Dahn, J. R. Combinatorial Investigations of Si-M (M=Cr+ Ni, Fe, Mn) Thin Film Negative Electrode Materials. *Electrochem. Solid-State Lett.* **2005**, 8 (2), A137–A140.
- (15) Todd, A. D. W.; Mar, R. E.; Dahn, J. R. Tin-Transition Metal-Carbon Systems for Lithium-Ion Battery Negative Electrodes. *J. Electrochem. Soc.* **2007**, *154* (6), A597-

A604.

- (16) Thorne, J. S.; Sanderson, R. J.; Dahn, J. R.; Dunlap, R. A. Combinatorial Study of the Sn–Cu–C System for Li-Ion Battery Negative Electrode Materials. *J. Electrochem. Soc.* **2010**, *157* (10), A1085–A1091.
- (17) Al-Maghrabi, M. A.; Thorne, J. S.; Sanderson, R. J.; Byers, J. N.; Dahn, J. R.; Dunlap, R. A. A Combinatorial Study of the Sn-Si-C System for Li-Ion Battery Applications. *J. Electrochem. Soc.* **2012**, *159* (6), A711–A719.
- (18) MacEachern, L.; Dunlap, R. A.; Obrovac, M. N. A Combinatorial Investigation of Fe-Si-Zn Thin Film Negative Electrodes for Li-Ion Batteries. *J. Electrochem. Soc.* **2015**, *162* (1), A229–A234.
- (19) Spong, A. D.; Vitins, G.; Guerin, S.; Hayden, B. E.; Russell, A. E.; Owen, J. R. Combinatorial Arrays and Parallel Screening for Positive Electrode Discovery. *J. Power Sources* **2003**, *119–121*, 778–783.
- (20) Roberts, M. R.; Spong, A. D.; Vitins, G.; Owen, J. R. High Throughput Screening of the Effect of Carbon Coating in LiFePO4 Electrodes. *J. Electrochem. Soc.* **2007**, *154* (10), A921–A928.
- (21) Roberts, M. R.; Vitins, G.; Owen, J. R. High-Throughput Studies of Li1– XMgx/2FePO4 and LiFe1– YMgyPO4 and the Effect of Carbon Coating. *J. Power Sources* **2008**, *179* (2), 754–762.
- (22) Kim, D.; Shim, H. C.; Yun, T. G.; Hyun, S.; Han, S. M. High Throughput Combinatorial Analysis of Mechanical and Electrochemical Properties of Li [NixCoyMnz] O2 Cathode. *Extrem. Mech. Lett.* **2016**, *9*, 439–448.
- (23) Liu, P.; Guo, B.; An, T.; Fang, H.; Zhu, G.; Jiang, C.; Jiang, X. High Throughput Materials Research and Development for Lithium Ion Batteries. *J. Mater.* **2017**, *3* (3), 202–208.
- (24) Fleischauer, M. D.; Hatchard, T. D.; Rockwell, G. P.; Topple, J. M.; Trussler, S.; Jericho, S. K.; Jericho, M. H.; Dahn, J. R. Design and Testing of a 64-Channel Combinatorial Electrochemical Cell. *J. Electrochem. Soc.* **2003**, *150* (11), A1465–A1469.
- (25) Dai, X.; Zhou, A.; Xu, J.; Yang, B.; Wang, L.; Li, J. Superior Electrochemical Performance of LiCoO2 Electrodes Enabled by Conductive Al2O3-Doped ZnO Coating via Magnetron Sputtering. *J. Power Sources* **2015**, 298, 114–122.
- (26) Li, X.; Liu, J.; Banis, M. N.; Lushington, A.; Li, R.; Cai, M.; Sun, X. Atomic Layer Deposition of Solid-State Electrolyte Coated Cathode Materials with Superior High-Voltage Cycling Behavior for Lithium Ion Battery Application. *Energy Environ. Sci.* **2014**, 7 (2), 768–778.
- (27) Dominko, R.; Gaberscek, M.; Drofenik, J.; Bele, M.; Pejovnik, S.; Jamnik, J. The Role of Carbon Black Distribution in Cathodes for Li Ion Batteries. *J. Power Sources* **2003**, *119–121*, 770–773.
- (28) David, L.; Thomas, B. R. Handbook of Batteries; McGraw-Hill Professional, 2001.

- (29) Lim, J.; Choi, A.; Kim, H.; Doo, S. W.; Park, Y.; Lee, K. T. In Situ Electrochemical Surface Modification for High-Voltage LiCoO2 in Lithium Ion Batteries. *J. Power Sources* **2019**, 426, 162–168.
- (30) Di Lecce, D.; Andreotti, P.; Boni, M.; Gasparro, G.; Rizzati, G.; Hwang, J.-Y.; Sun, Y.-K.; Hassoun, J. Multiwalled Carbon Nanotubes Anode in Lithium-Ion Battery with LiCoO2, Li[Ni1/3Co1/3Mn1/3]O2 and LiFe1/4Mn1/2Co1/4PO4 Cathodes. ACS Sustain. Chem. Eng. 2018, 6.
- (31) Shaju, K. M.; Subba Rao, G. V; Chowdari, B. V. R. Performance of Layered Li(Ni1/3Co1/3Mn1/3)O2 as Cathode for Li-Ion Batteries. *Electrochim. Acta* **2002**, *48* (2), 145–151.
- (32) Lu, Z.; Beaulieu, L. Y.; Donaberger, R. A.; Thomas, C. L.; Dahn, J. R. Synthesis, Structure, and Electrochemical Behavior of Li [Ni x Li1/3- 2x/3Mn2/3- x/3] O 2. *J. Electrochem. Soc.* **2002**, *149* (6), A778–A791.
- (33) Zhang, X.; Meng, X.; Elam, J. W.; Belharouak, I. Electrochemical Characterization of Voltage Fade of Li1.2Ni0.2Mn0.6O2 Cathode. *Solid State Ionics* **2014**, *268*, 231–235.
- (34) Rozier, P.; Tarascon, J. M. Li-Rich Layered Oxide Cathodes for next-Generation Li-Ion Batteries: Chances and Challenges. *J. Electrochem. Soc.* **2015**, *162* (14), A2490–A2499.
- (35) Cabana, J.; Kang, S.-H.; Johnson, C. S.; Thackeray, M. M.; Grey, C. P. Structural and Electrochemical Characterization of Composite Layered-Spinel Electrodes Containing Ni and Mn for Li-Ion Batteries. *J. Electrochem. Soc.* **2009**, *156* (9), A730–A736.
- (36) Gu, M.; Belharouak, I.; Zheng, J.; Wu, H.; Xiao, J.; Genc, A.; Amine, K.; Thevuthasan, S.; Baer, D. R.; Zhang, J.-G. Formation of the Spinel Phase in the Layered Composite Cathode Used in Li-Ion Batteries. *ACS Nano* **2012**, *7* (1), 760–767.

Table I. Summary of the electrochemical parameters for 32 samples of both LCO and NMC obtained here using the combinatorial cell, compared to results for bulk samples from the literature. ^{28–31} RSD is the relative standard deviation of the combinatorial capacities and average voltages.

Material	Discharge Capacity (mAhg ⁻¹)		RSD (%)	Average Voltage (V)		RSD (%)
	Combinatorial	Literature		Combinatorial	Literature	
LCO	163.5	155-165	7.57	3.96	3.9	0.45
NMC	151.0	155-160	7.80	3.78	3.8	0.65

Figure captions:

Figure 1. (A) Design of the printed circuit boards (PCB) (top), and cross-sectional view of the combinatorial cell (bottom). (B) Comparison of experimental (black) and literature^{25,26} (red) cyclic voltammograms of LCO and NMC. Combinatorial samples were cycled at a scan rate of 0.1 Vh⁻¹. Literature samples were cycled at a scan rate of 0.18 Vh⁻¹ and 0.36 Vh⁻¹ for LCO and NMC, respectively.

Figure 2. Cyclic voltammograms of LCO and NMC arranged in a checkerboard pattern in the combinatorial cell in the range 3.0 - 4.4 V at 0.1 Vh⁻¹. The shaded regions indicate NMC compositions, while the rest are LCO.

Figure 3. Li-Mn-Ni-O structural phase diagram⁹ along with the specific energies obtained here during discharge from 4.8 V to 3.0 V. Solid black lines are boundaries to single-phase regions, dashed black lines are tie-lines at the boundaries of triple-phase regions, and the dotted black line is the phase transition from rocksalt to the layered structure. S, L, and R are spinel, layered, and rocksalt, respectively. The red boxed insets show voltage vs. capacity curves for the first 2 cycles with all x-axes being from 0 to 400 mAh/g and all y-axes having the range 3.0 - 5.0 V. Similarly, all green boxed insets show the first cycle cyclic voltammograms with y-axes from -60 to 60 mA/g and x-axes in the range 3.0 to 5.0 V.

Figure 4. Li-Mn-Ni-O ternary maps of various electrochemical performance metrics on discharge. (A) Specific capacity for cycling performed between 3.0 and 4.4 V. (B) Specific capacity and (C) average voltage for cycling performed between 3.0 V and 4.8 V vs. Li/Li⁺. (D) Change in discharge voltage fade between cycles 3 and 4 (3.0 - 4.8 V range), a positive value indicates a decrease in average voltage in the later cycle.

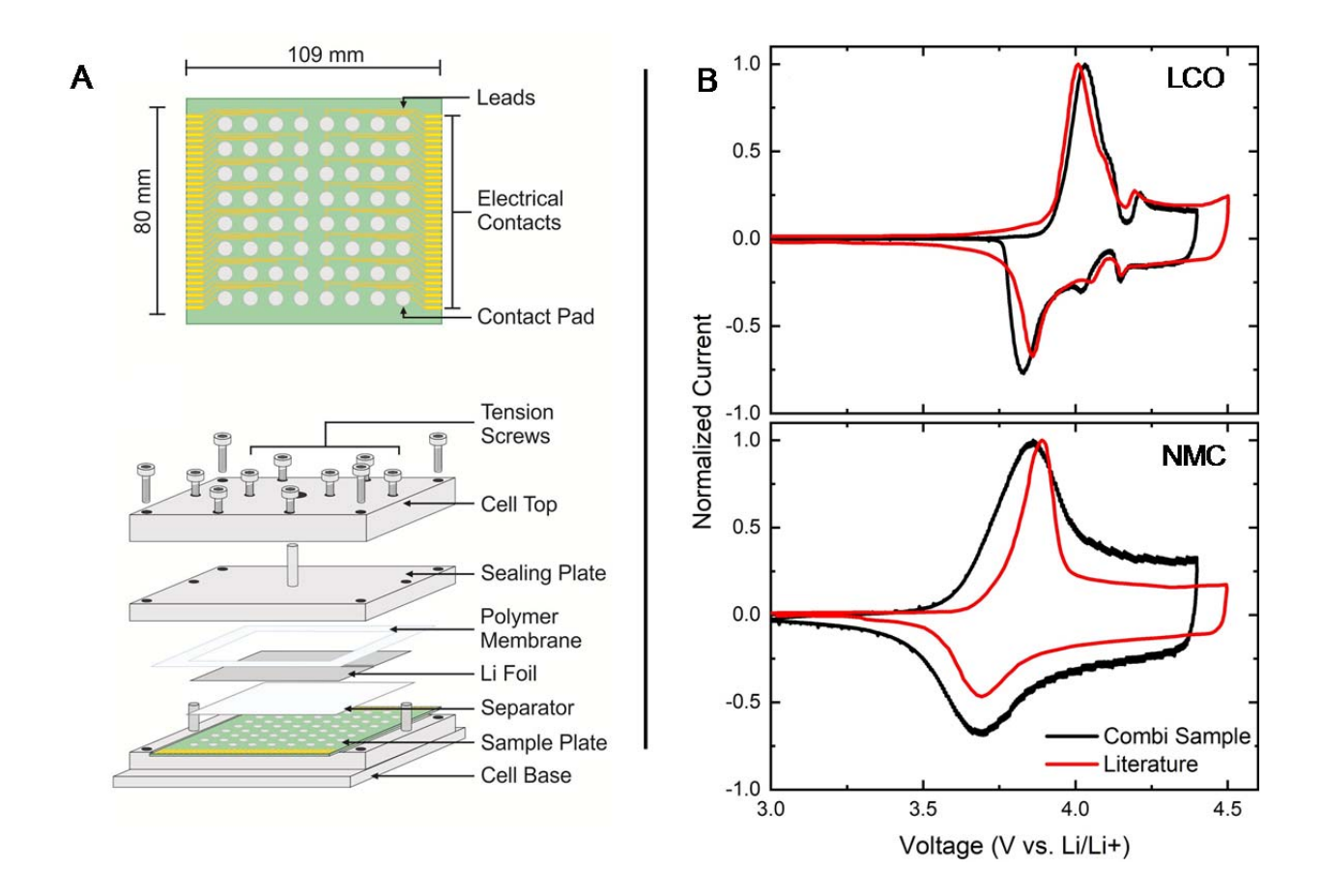


Figure 1.

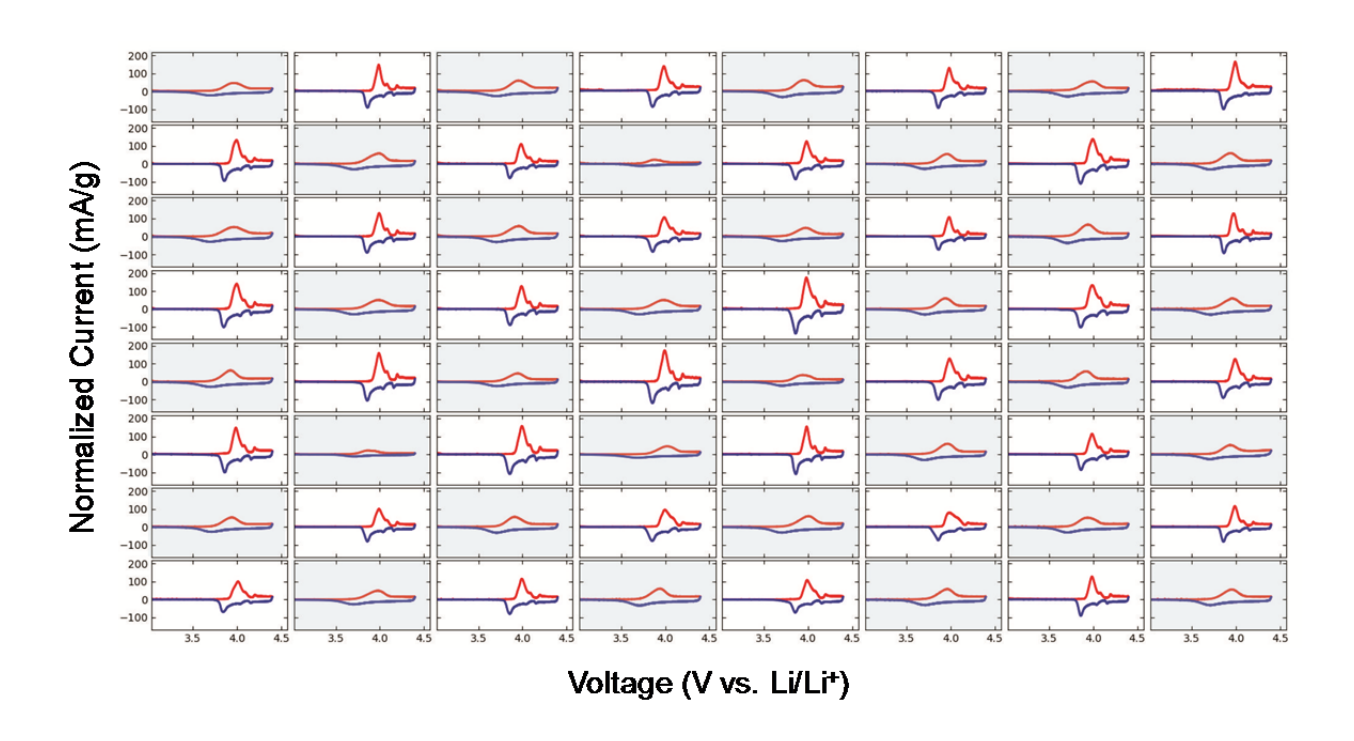


Figure 2.

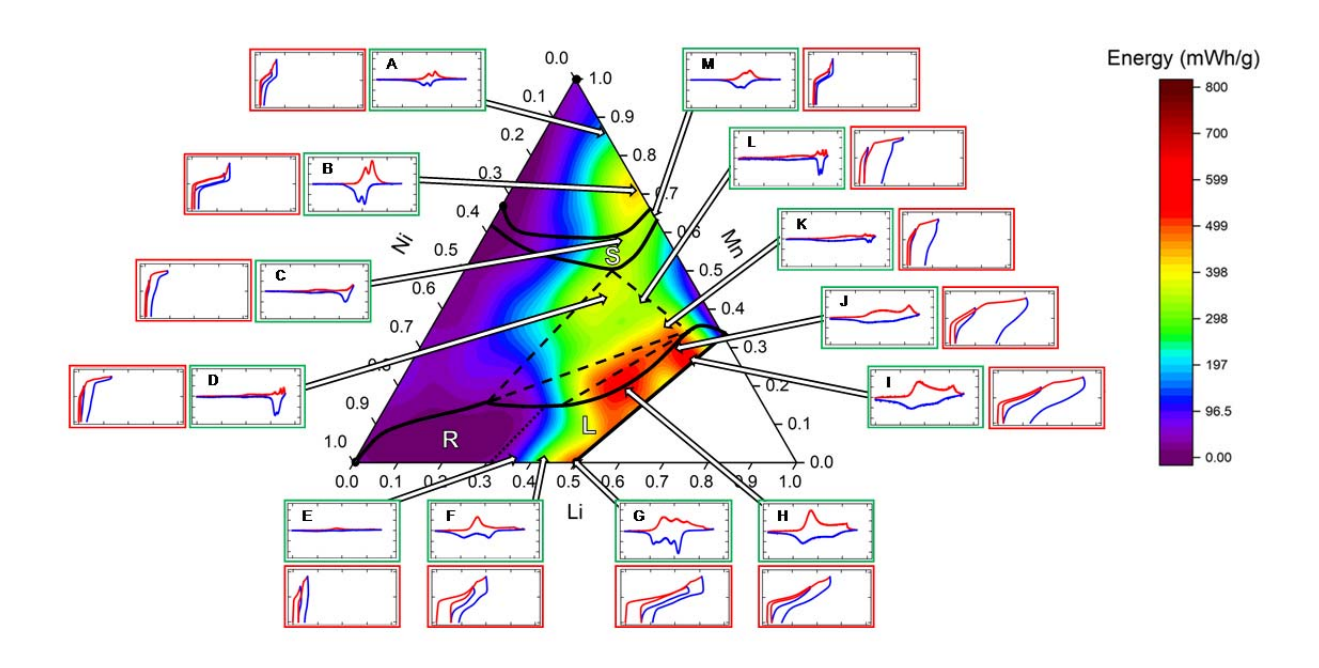


Figure 3.

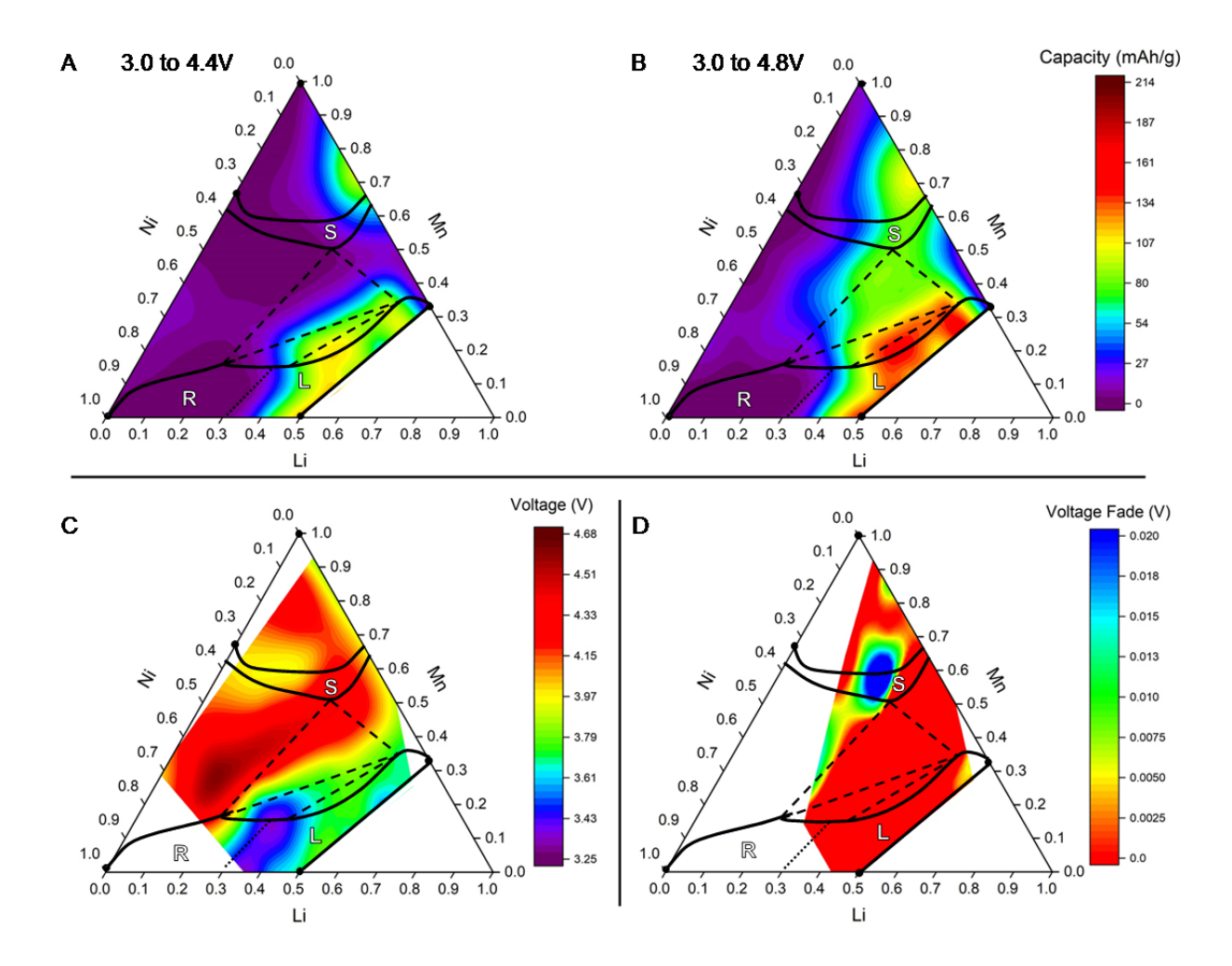


Figure 4.